

Transfer of nanopantography-defined patterns using highly selective plasma etching

Siyuan Tian,^{a)} Vincent M. Donnelly,^{b)} and Demetre J. Economou^{c)}

Plasma Processing Laboratory, Department of Chemical and Biomolecular Engineering, University of Houston, 4800 Calhoun Road, Houston, Texas 77204-4004

(Received 17 February 2015; accepted 9 April 2015; published 22 April 2015)

Nanopantography is a method for massively parallel patterning of nanofeatures over large areas. Transfer of patterns defined by nanopantography using highly selective plasma etching of Si, with the native silicon oxide as hard mask, can improve patterning speed and etch profile. With this method, arrays of high aspect ratio (>5) ~ 10 nm-diameter holes, as well as slots, were fabricated in silicon with no mask undercut. The ability to fabricate complex patterns using nanopantography, followed by highly selective plasma etching, was also demonstrated. © 2015 American Vacuum Society. [<http://dx.doi.org/10.1116/1.4918716>]

I. INTRODUCTION

Lithography at the sub-10 nm scale is essential for the fabrication of future integrated circuits, as well as a variety of other nanodevices. Extreme ultraviolet lithography, a contender for “next generation lithography,” has been delayed due to many issues, including low throughput and high cost.^{1,2} Block copolymer directed self-assembly can produce a limited variety of patterns with dimensions <10 nm.^{3–8} Nanoimprint lithography shows promise for low-cost, high-throughput fabrication, with ultimate resolution in the sub-10 nm regime, but because it is a contact process, defect reduction has slowed its introduction to manufacturing.^{9–12} Ion or electron beam proximity or projection lithographies can define features finer than 20 nm, but proximity printing requires fragile stencil masks with equally fine features,¹³ and projection printing needs large field optics and is subject to Coulomb interaction limitations.¹⁴ Multiple e-beam lithography integrates tens of thousands of 5 keV-electron beams for parallel writing, but has demonstrated a resolution of only 32 nm at present.^{15,16} Scanning probe lithography can achieve sub-10 nm resolution, but this method is too slow for large area fabrication.^{17–20}

Nanopantography is a new patterning method for massively parallel writing of nanofeatures over large areas. Billions of electrostatic lenses are first fabricated on top of a wafer using conventional semiconductor manufacturing processes. A broad area, collimated, monoenergetic ion beam is then directed toward the wafer surface. By applying an appropriate DC voltage to the lens array with respect to the wafer, the ion beamlet entering each lens converges to a fine spot focused on the wafer surface that can be $100\times$ smaller than the diameter of the lens.^{21,22} By controlling the tilt of the substrate with respect to the ion beam, the focused ion beamlets can “write” a desired pattern in a massively parallel fashion in selected areas of the substrate.

Nanopantography has been employed to etch 10 nm-diameter holes in Si by simultaneous exposure to a

monoenergetic Ar^+ ion beam and Cl_2 gas.²¹ Etching of trenches and more complex patterns was also demonstrated.²² Throughput was a challenge, however. For example, it took 30 min to etch an array of 50 nm-diameter, 100-nm deep holes in Si. Another issue was that etched features showed an unwanted tapered sidewall at an angle that depended on the numerical aperture of the lens. This also resulted in a size of the etched feature at the wafer surface that was larger than the inherent resolution of the technique.

A two-step process in which very shallow patterns are defined in an ultrathin mask by nanopantography, and then transferred into an underlying material by highly selective plasma etching, would greatly improve throughput. Recently, it was found that p-type Si could be etched in chlorine-containing plasmas with ion energies below the ion-assisted etching threshold (<16 eV).^{23,24} This sub-threshold etching was shown to be due to photons (especially in the VUV) emanating from the plasma. There was little or no isotropic etching of p-type silicon under the conditions studied, i.e., no undercut was observed in the etch profiles. With such low ion energy, while maintaining a moderate etching rate of Si (tens of nm/min), it should be possible to use an ultrathin mask, such as the native oxide on Si, to transfer a nanopantography-defined pattern deep into the Si substrate with minimal or no mask undercut.

In this letter, we demonstrate this new method to transfer nanopantography-defined patterns using highly selective plasma etching. The process flow is schematically depicted in Fig. 1. In the first step, a desired pattern is defined on a Si wafer using nanopantography with a short exposure time (typically 3 min). The purpose is not to etch deep into silicon, but to break through the native oxide on top of silicon, creating a shallow pattern on the wafer surface that can serve as mask. In the second step, the pattern is transferred into the Si wafer, using a chlorine plasma under photo-assisted etching conditions (subthreshold ion energies). Because of the very low ion energy, the selectivity of etching silicon over silicon dioxide is very high (~ 120), allowing high aspect ratio features (>5) to be formed in Si, despite the very thin mask.

^{a)}Present address: Lam Research Corp., Fremont, CA 94538.

^{b)}Electronic mail: vmdonnelly@uh.edu

^{c)}Electronic mail: economou@uh.edu

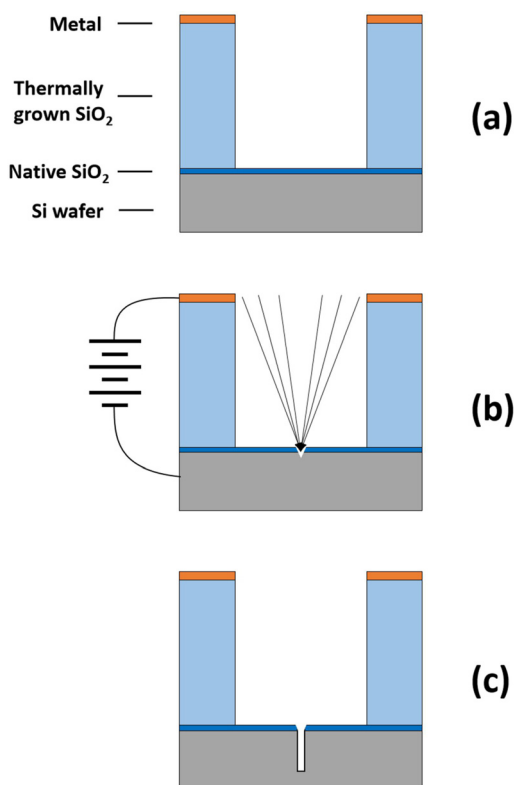


FIG. 1. (Color online) Transfer of patterns defined by nanopantography using highly selective plasma etching: (a) Schematic of lens structure. (b) A DC potential is applied between the metal and the silicon wafer to focus the ion beamlet. A shallow pattern is formed by nanopantographic etching of the native oxide of silicon using a focused Ar^+ ion beam and Cl_2 gas. (c) Pattern formed in (b) is transferred deep into silicon by highly selective chlorine plasma etching using native oxide of silicon as a hard mask.

II. EXPERIMENT

The nanopantography apparatus was the same as that described by Xu *et al.*,²² except that a new high density inductively coupled plasma source was installed to achieve higher beam current with a narrower ion angular distribution. Monoenergetic ions were extracted through a grid using a pulsed plasma technique.²⁵ Ions traveled to the sample, 60 cm downstream from the extraction grid, drifting through a region that was differentially pumped (pressure = 5×10^{-6} Torr during processing) to minimize collisions with the background gas.

Electrostatic lenses were fabricated on a Si substrate using standard semiconductor manufacturing techniques. The lens structure is shown in Fig. 1(a). A 150 nm sputter deposited Al layer was separated from the p-Si substrate by 1000 nm of thermally grown oxide. The metal-oxide-silicon structure comprises an electrostatic lens that focuses the ion beamlets entering the structure. The lenses used in this work had a diameter of 650 nm and a focal length of 1150 nm (150 nm Al + 1000 nm SiO_2). The lens array had a pitch of $1.15 \mu\text{m}$ in both x and y directions, over a $2 \times 5 \text{mm}^2$ area of the sample, which corresponded to a total of 7.5×10^6 lenses.

During the last step of the lens fabrication process, SiO_2 etching with Al as the mask, SiO_2 was completely removed

by over-etching, exposing the Si underneath. After fabrication, lenses were exposed to ambient air, forming a native oxide with a saturated thickness of $\sim 16\text{--}20 \text{ \AA}$.^{26,27} For such a thin oxide layer, any charge deposited on the surface by the ion beam is expected to be neutralized by a leakage current to the substrate, thus avoiding charging of the oxide, which would lower the energy of the ion beam striking the substrate and distort the ion focus.

Si substrates patterned with the electrostatic lens arrays described above were loaded into the nanopantography processing chamber, and oriented perpendicular to the ion beam direction. The Si substrate was electrically connected to ground, while the Al layer on top was DC biased with the optimum voltage of 96.8 V, determined by experiments and simulations to yield the minimum focal spot size of Ar^+ , with the measured ion energy of 107 eV. Cl_2 was then admitted into the processing chamber through a leak valve such that the pressure in the processing chamber was 3.0×10^{-5} Torr. (The base pressure was 1.0×10^{-7} Torr.) The nearly monoenergetic (3 eV FWHM) Ar^+ beam was extracted from a pulsed inductively coupled plasma using synchronized bias on a boundary electrode.²⁵ The ion beam current density at the sample location was measured to be $1 \mu\text{A}/\text{cm}^2$. The substrate holder could be tilted independently in two dimensions with a computer controlled accuracy of $\pm 0.015^\circ$, allowing writing of any arbitrary, non-reentrant pattern. After etching nanopatterns through the native oxide, to expose the underlying silicon, the sample was taken out of the nanopantography apparatus and was quickly transferred to the plasma etching reactor. During the less than 5 min exposure to ambient air, one would expect no more than a few monolayers of oxide regrowing on the silicon surface.

Chlorine plasma etching was carried out in a Tokyo Electron Radial Line Slot Antenna (RLSA[®]) reactor. The 1500 W microwave excited plasma has a very low electron temperature ($T_e \sim 1 \text{ eV}$ at 5 mTorr) above the wafer, as determined by Langmuir probe analysis.²⁸ With no RF bias on the electrically floating wafer stage, the ion bombardment energy is expected to be $\sim 5T_e$,²⁹ and therefore below the threshold for ion-assisted etching of silicon.

Silicon samples were mounted, using Fomblin[®] oil, at the center of a 200 mm diameter silicon wafer that was positioned 40 cm below the quartz window through which the microwaves were fed. Samples with a lens structure fabricated on them, but not exposed to nanopantography, were used to measure the Si etching rate and ascertain the plasma etch resistance of the native oxide of silicon under the chosen plasma conditions. An induction period of about 7 min was observed before Si etching commenced, corresponding to breaking through the native oxide. After this induction period, silicon etched at a constant rate of $\sim 30 \text{ nm}/\text{min}$. After plasma etching, samples were cleaved and examined by scanning electron microscopy.

III. RESULTS AND DISCUSSION

A feasibility experiment was carried out by forming a hole at the center of the bottom of each lens. The focusing

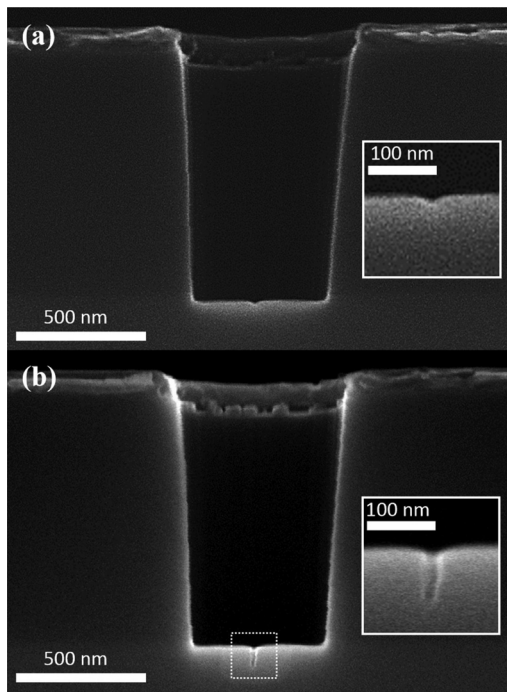


FIG. 2. Hole etched in silicon using the present method of pattern transfer. After plasma etching, hole surface diameter and depth are 15 and 80 nm, respectively.

voltage was set at 96.8 V. For a nanopantography process time of 3 min, the silicon was etched less than 10-nm-deep [Fig. 2(a)]. After chlorine plasma etching for 7 min, using the parameter values given above, the hole was 80 nm deep, while the rest of Si surface was successfully protected by the native oxide [Fig. 2(b)]. With an etching rate of 30 nm/min, it would be expected to take only 2.7 min to etch Si to a depth of 80 nm. It is possible that upon air exposure, a few monolayers of native oxide reformed in the spots cleared by nanopantography, requiring 4.3 min to be removed in the chlorine plasma. We have observed, however, that the etching rate slows down with time in small features, leading to the more likely conclusion that aspect ratio dependent etching limits the depth of these features.

Lines were also written by nanopantography, using the optimum focusing voltage of 96.8 V and a 50 s dwell time

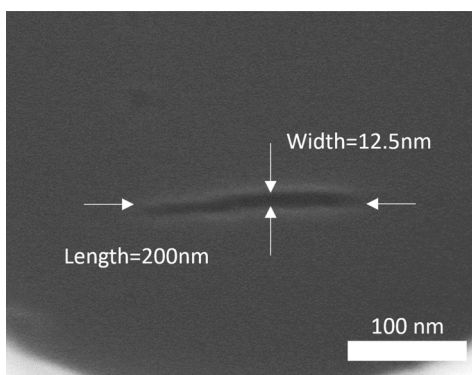


FIG. 3. 12.5-nm-wide, 200-nm-long line etched in silicon using the present method of pattern transfer. The depth was 80 nm (aspect ratio > 6). Scale bar is 100 nm.

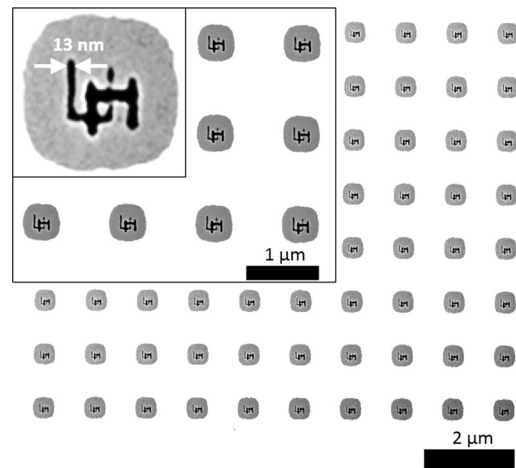


FIG. 4. Interlocking “UH” logo etched in silicon using the present method of pattern transfer. Only 80 of the 7.5×10^6 lenses are shown. The thinnest line is ~ 13 nm.

per exposure step. The exposure step size was 3.4 nm, achieved by tilting the sample stage $0.17^\circ/\text{step}$. The equivalent writing speed is 4.1 nm/min. A 200-nm-long trench with 12.5 nm width was obtained using chlorine plasma etching after nanopantography patterning (Fig. 3). The depth of the Si trench was ~ 80 nm, resulting in an aspect ratio (depth/width) of 6.4. Since there are 7.5×10^6 lenses on the wafer, the overall writing speed is 3 cm/min. This speed can be readily increased to 160 cm/min by fabricating 400×10^6 lenses with $1 \mu\text{m}$ pitch, over an area of $2 \text{ cm} \times 2 \text{ cm}$. These values can be compared to the 10 cm/h e-beam writing speed for similarly sized (~ 10 nm) features.^{30–32}

Finally, interlocking “UH” logos were written over $225 \text{ nm} \times 250 \text{ nm}$ areas with an exposure step size of 3.4 nm and dwell time of 50 s (Fig. 4). The thinnest line near the crossing point of the right vertical line of letter “U” and the horizontal line of letter “H” is ~ 13 nm-wide.

Using highly selective chlorine plasma etching to transfer patterns, defined by nanopantography, results in improvement in both writing speed and feature resolution. Instead of etching a 100-nm-deep feature in Si, only a 1–2 nm of SiO_2 needs to be removed, and this reduces the nanopantography process time from 30 min to 50 s. In addition, the resolution is improved because a much thinner layer of material has to be removed by nanopantography. Because the ion beam focus spot is only 6–7 nm (based on the smallest feature obtained) roughly equal to the FWHM of 8 nm found in simulations for this lens diameter and numerical aperture $\text{NA} = 0.28$, the depth of focus (DOF) of the beam is shallow, i.e., only ~ 20 nm.³³ Etching beyond the range of the DOF would create features larger than the focal spot size, degrading the inherent resolution. By reducing the etched thickness to a few nanometers, the etched layer completely falls into the DOF of the ion beamlets, resulting in better resolution.

IV. SUMMARY AND CONCLUSIONS

In summary, transfer of patterns defined by nanopantography was demonstrated using highly selective chlorine plasma etching. The native oxide of silicon served as a hard mask,

due to the high selectivity of chlorine plasma etching with subthreshold ion bombardment energies. High aspect ratio (>5) nanopatterns with ~10 nm openings were fabricated in silicon with no mask undercut. An array of “UH” logos with ~13 nm-wide nanoletters was fabricated to demonstrate the ability to fabricate arbitrary, non-reentrant patterns, using nanopantography, followed by highly selective plasma etching. The smallest features fabricated so far by this method were 6 nm diameter holes.

ACKNOWLEDGMENTS

Financial support by the National Science Foundation grant CMMI 1030620 is gratefully acknowledged. Thanks to V. Samara of the University of Houston for his help with plasma etching.

- ¹J. V. Hermans, D. Laidler, P. Foubert, K. D'Havé, S. Cheng, M. Dusa, and E. Hendrickx, *Proc. SPIE* **8322**, 832202 (2012).
- ²A. Mallik *et al.*, *Proc. SPIE* **9048**, 90481R (2014).
- ³R. Ruiz, H. Kang, F. A. Detcheverry, E. Dobisz, D. S. Kercher, T. R. Albrecht, J. J. de Pablo, and P. F. Nealey, *Science* **321**, 936 (2008).
- ⁴P. Rincon Delgadillo, R. Harukawa, M. Suri, S. Durant, A. Cross, V. R. Nagaswami, D. Van Den Heuvel, R. Gronheid, and P. Nealey, *Proc. SPIE* **8680**, 86800L (2013).
- ⁵R. A. Farrell *et al.*, *Proc. SPIE* **9051**, 90510Z (2014).
- ⁶S.-M. Park, X. Liang, B. D. Harteneck, T. E. Pick, N. Hiroshiba, Y. Wu, B. A. Helms, and D. L. Olynick, *ACS Nano* **5**, 8523 (2011).
- ⁷D. J. C. Herr, *J. Mater. Res.* **26**, 122 (2011).
- ⁸J. G. Son, J.-B. Chang, K. K. Berggren, and C. A. Ross, *Nano Lett.* **11**, 5079 (2011).
- ⁹S. Y. Chou, P. R. Krauss, and P. J. Renstrom, *J. Vac. Sci. Technol., B* **14**, 4129 (1996).
- ¹⁰F. Hua *et al.*, *Nano Lett.* **4**, 2467 (2004).
- ¹¹R. F. Pease and S. Y. Chou, *Proc. IEEE* **96**, 248 (2008).
- ¹²T. Higashiki, T. Nakasugi, and I. Yoneda, *J. Micro/Nanolithogr. MEMS MOEMS* **10**, 043008 (2011).
- ¹³R. S. Dhaliwal *et al.*, *IBM J. Res. Dev.* **45**, 615 (2001).
- ¹⁴E. Platzgummer, *Proc. SPIE* **7637**, 763703 (2010).
- ¹⁵M. J. Wieland *et al.*, *Proc. SPIE* **7637**, 76370F (2010).
- ¹⁶G. de Boer, M. P. Dansberg, R. Jager, J. J. M. Peijster, E. Slot, S. W. H. K. Steenbrink, and M. J. Wieland, *Proc. SPIE* **8680**, 86800O (2013).
- ¹⁷D. Pires, J. L. Hedrick, A. De Silva, J. Frommer, B. Gotsmann, H. Wolf, M. Despont, U. Duerig, and A. W. Knoll, *Science* **328**, 732 (2010).
- ¹⁸L. L. Cheong, P. Paul, F. Holzner, M. Despont, D. J. Coady, J. L. Hedrick, R. Allen, A. W. Knoll, and U. Duerig, *Nano Lett.* **13**, 4485 (2013).
- ¹⁹A. W. Knoll *et al.*, *Proc. SPIE* **9049**, 90490B (2014).
- ²⁰M. Kaestner and I. W. Rangelow, *J. Vac. Sci. Technol., B* **29**, 06FD02 (2011).
- ²¹L. Xu, S. C. Vemula, M. Jain, S. K. Nam, V. M. Donnelly, D. J. Economou, and P. Ruchhoeft, *Nano Lett.* **5**, 2563 (2005).
- ²²L. Xu, A. Nasrullah, Z. Chen, M. Jain, P. Ruchhoeft, D. J. Economou, and V. M. Donnelly, *Appl. Phys. Lett.* **92**, 013124 (2008).
- ²³H. Shin, W. Zhu, V. M. Donnelly, and D. J. Economou, *J. Vac. Sci. Technol., A* **30**, 021306 (2012).
- ²⁴W. Zhu, S. Sridhar, L. Liu, E. Hernandez, V. M. Donnelly, and D. J. Economou, *J. Appl. Phys.* **115**, 203303 (2014).
- ²⁵L. Xu, D. J. Economou, V. M. Donnelly, and P. Ruchhoeft, *Appl. Phys. Lett.* **87**, 041502 (2005).
- ²⁶S. I. Raider, R. Flitsch, and M. J. Palmer, *J. Electrochem. Soc.* **122**, 413 (1975).
- ²⁷U. Satoshi, F. Masanori, H. Hideki, and N. Naoto, *Jpn. J. Appl. Phys., Part 1* **40**, 5312 (2001).
- ²⁸C. Tian, T. Nozawa, K. Ishibasi, H. Kameyama, and T. Morimoto, *J. Vac. Sci. Technol., A* **24**, 1421 (2006).
- ²⁹M. A. Lieberman and A. J. Lichtenberg, *Principles of Plasma Discharges and Materials Processing*, 2nd ed. (Wiley, New York, 2005).
- ³⁰C. Vieu, F. Carcenac, A. P  pin, Y. Chen, M. Mejias, A. Lebib, L. Manin-Ferlazzo, L. Couraud, and H. Launois, *Appl. Surf. Sci.* **164**, 111 (2000).
- ³¹H. Duan, V. R. Manfrinato, J. K. W. Yang, D. Winston, B. M. Cord, and K. K. Berggren, *J. Vac. Sci. Technol., B* **28**, C6H11 (2010).
- ³²A. E. Grigorescu and C. W. Hagen, *Nanotechnology* **20**, 292001 (2009).
- ³³J. Orloff, *Handbook of Charged Particle Optics*, 2nd ed. (CRC, Boca Raton, FL, 2008), pp. 437–496.